Redox Properties of Human Transferrin Bound to Its Receptor†

Suraj Dhungana,§ Céline H. Taboy,§ Olga Zak,‡ Mykol Larvie,|| Alvin L. Crumbliss,§ and Philip Aisen*,‡

Department of Physiology and Biophysics, Albert Einstein College of Medicine, 1300 Morris Park Avenue, Bronx, New York 10461, Department of Chemistry, Duke University, Box 90346, Durham, North Carolina 27708-0346, and Harvard-MIT Division of Health Sciences and Technology, Cambridge, Massachusetts 02139

Received July 31, 2003; Revised Manuscript Received November 5, 2003

ABSTRACT: Virtually all organisms require iron, and iron-dependent cells of vertebrates (and some more ancient species) depend on the Fe^{3+}-binding protein of the circulation, transferrin, to meet their needs. In its iron-donating cycle, transferrin is first captured by the transferrin receptor on the cell membrane, and then internalized to a proton-pumping endosome where iron is released. Iron exits the endosome to enter the cytoplasm via the ferrous iron transporter DMT1, a molecule that accepts only Fe^{2+}, but the reduction potential of ferric iron in free transferrin at endosomal pH (∼5.6) is below −500 mV, too low for reduction by physiological agents such as the reduced pyridine nucleotides with reduction potentials of −284 mV. We now show that in its complex with the transferrin receptor, which persists throughout the transferrin-to-cell cycle of iron uptake, the potential is raised by more than 200 mV. Reductive release of iron from transferrin, which binds Fe^{2+} very weakly, is therefore physiologically feasible, a further indication that the transferrin receptor is more than a passive conveyor of transferrin and its iron.

Transferrin (Tf),[1] the iron transporter of circulating blood, is a single-chain, bilobal protein with a single Fe^{3+} binding site in each lobe. Iron is borne by Tf only as Fe^{3+}, with a reduction potential too low (<−500 mV) for it to be reduced to Fe^{2+} by physiological means, either at extracellular pH (7.4) or at endosomal pH (near 5.6) (*1*, *2*). The initial event in the uptake of transferrin-borne iron by cells is the binding of the protein to specific transferrin receptors, of which two are known: TfR1 (or, more simply, TfR in keeping with its status as the first discovered and most intensively studied) and the recently discovered TfR2 (*3*), of still uncertain function; our present concern is confined to TfR1. The membrane segment bearing the complex of transferrin and TfR is then internalized by the iron-requiring cell to an ATP-driven proton-pumping endosome, where the pH is lowered to a range of 5.4−6.0 (*4*, *5*). After release from Tf, iron exits the endosome via the membrane divalent metal ion transporter now known as DMT1 (*6*), which accepts iron only as Fe^{2+}. Where in the transferrin-to-cell cycle in iron metabolism reduction of iron occurs is not known. Although iron released from Tf to most physiological iron binders is easily reducible (*7*), the time required for release from transferrin of iron as Fe^{3+} to physiological chelators, even at endosomal pH, is long (>6 min) compared to the cell-cycling time of transferrin, which may be as little as 1−2 min (*8*). Transferrin completes some 100−200 cycles of iron uptake, transport, and delivery to cells during its lifetime in the circulation (*9*). A fundamental and still unanswered question in iron metabolism, then, is how iron is released from Tf and reduced to the ferrous state for passage across the endosomal membrane to the cytoplasm in meeting the needs of iron-requiring cells. After completing its iron-donating function, transferrin leaves the cell, depleted of iron but otherwise intact, for another cycle of iron transport and delivery. A salient feature of the transferrin-to-cell endocytic cycle in iron metabolism is the persistence of the Tf/TfR assembly throughout the cycle: transferrin free of its receptor is not known to exist within the cell. Although iron-free apoTf is bound weakly, if at all, to TfR at extracellular pH, the relative affinity of the receptor may be greater for iron-free than for iron-bearing Tf at endosomal pH (*10*). Thus, TfR may provide a thermodynamic drive to the reduction of Fe^{3+} in transferrin. An attractive hypothesis, supported by consideration of the thermodynamics and kinetics of iron chelation, is that Fe^{3+} reduction occurs while iron is still bound to transferrin. Reduction to Fe^{2+} diminishes the affinity of transferrin for iron by at least a factor of 10^{14} (*11*) and taking water ligand exchange rates for $Fe(H_2O)_6^{3+}$ and $Fe(H_2O)_6^{2+}$ as an indicator, will enhance first coordination shell turnover kinetics by several orders of magnitude (*12*, *13*). The possibility that binding of transferrin to its receptor modulates the reduction potential of transferrin-bound iron, as it does the release of Fe^{3+} from transferrin (*14*), was therefore investigated.

MATERIALS AND METHODS

Experimental Design. The reduction potentials of iron in the C-terminal lobe of transferrin complexed to receptor, at extracellular pH (7.4) and at endosomal pH (5.8), were

* To whom correspondence should be addressed. Phone: (718) 430−2593. Fax: (718) 430−8819. E-mail, aisen@aecom.yu.edu.

† This work was supported in part by Grants DK15056 from the National Institutes of Health, U.S. Public Health Service (PA), and CHE-0079066 from the National Science Foundation (ALC).

‡ Albert Einstein College of Medicine.

§ Duke University.

|| Harvard-MIT.

[1] Abbreviations: Tf, human transferrin; TfR, transferrin receptor; OTTLE, optically transparent thin-layer electrochemical cell; NHE, normal hydrogen electrode; DMT1, divalent metal transporter 1; MV, methyl viologen; C-lobe, the C-terminal lobe of transferrin (residues 334−679); N-lobe, the N-terminal lobe of transferrin (residues 1−337); Fe_C, Fe bound to C-lobe; Fe_C/TfR, Fe in C-lobe complexed to transferrin receptor; Tf/TfR, the complex of transferrin with receptor; FeTf, iron in either lobe or both lobes of Tf.

10.1021/bi0353631 CCC: $27.50
Published on Web 12/09/2003

measured by a spectroelectrochemical method as previously described (*2*). Because of uncertain results with full-length diferric transferrin (see below), we also chose to study isolated C-lobe to avoid confounding effects of migration, release, and reduction of iron carried by the N-lobe of transferrin, where it is bound much more weakly at endosomal pH than in the C-lobe. Furthermore, most of the binding energy in the complex of transferrin with its receptor is derived from the C-lobe (*15*), so that effects of receptor might be more clearly displayed in iron bound to that lobe.

Proteins and Complexes. Human serum transferrin saturated with Fe^{3+} was obtained from Boehringer-Mannheim (Indianapolis, IN). Recombinant C-lobe in verified native configuration was prepared by previously described methods (*15*, *16*). The soluble exocytic portion of TfR was expressed and purified as described by Lawrence et al. (*17*), or provided by Dr. Peter Snow of the California Institute of Technology (*18*). Complexes of iron-bearing Tf or C-lobe and receptor were prepared by incubating a 2-fold molar excess of either protein with receptor. After 1−2 h incubation at 37 °C and overnight at 4 °C in 0.05 M HEPES/0.1 M NaCl, pH 7.4, size exclusion chromatography on a Superdex 200 16/60 column (Pharmacia, Piscataway, NJ) separated assemblies from unbound proteins. Preparations were maintained at 4 °C before exchange to working buffers, 0.05 M MOPS/0.5 M KCl, pH 7.0 or 0.05 M MES/0.5 M KCl, pH 5.8, each with 0.2−0.4 mM methyl viologen as electrochemical mediator to shuttle electrons between the electrode and the redox-active site buried within the protein. The high concentration of salt as supporting electrolyte was needed to achieve equilibrium of Fe^{3+}/Fe^{2+} in reasonable times as applied potentials were varied. The concentrations of transferrin or C-lobe in their complexes with receptor were in the range of 0.1 to 0.2 mM.

Spectroscopy. Visible spectra were recorded during the course of spectroelectrochemical studies in the OTTLE cell previously described (*2*). EPR spectra were obtained with a Bruker 200 D X-band spectrometer with ESP 300 upgrade and VT 4111 temperature controller. Instrumental settings: temperature, 100 K; microwave power, 10 mW; microwave frequency, 9.514 GHz; modulation amplitude, 1 mT.

RESULTS

Characterization of Receptor Complexes. Optical spectra of receptor complexes of diferric transferrin and C-lobe showed the characteristic broad absorption bands centered at 465 nm arising from ligand-to-metal charge transfer between electronegative oxygen donors of ligand tyrosinates and Fe^{3+} at the specific binding sites of transferrin and C-lobe (Figure 1). The intensity of these bands declined as more negative potentials were applied, but did not qualitatively change in their overall features. An EPR spectrum of the C-lobe/TfR complex at pH 5.8, recovered from the OTTLE cell after completion of spectroelectrochemical studies, was also unperturbed relative to C-lobe in the principal features of the $g' = 4.3$ line, including the characteristic splitting near 4.1 mT (Figure 2). The broad hump at the low-field side of the line is attributed to the high salt content of the spectroelectrochemical buffer (*19*). We conclude that the first coordination shell of Fe^{3+} in transferrin is intact and unperturbed when C-lobe is complexed with TfR. Consequently, we assume that C-lobe and C-lobe/TfR complex

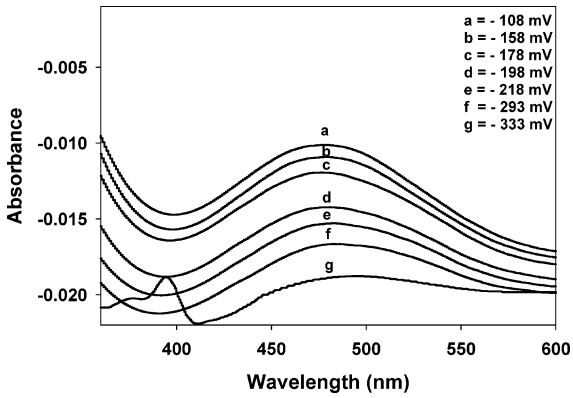

FIGURE 1: Visible spectra of Fe_C/TfR during the course of a typical electrochemical reduction. Conditions: buffer, 50 mM MES, 500 mM KCl, pH 5.8; [Fe_C/TfR] = 0.19 mM; [MV^+] = 1.4 mM. The absorbance peak at <400 nm in trace g is due to the reduced form of the mediator which appears at low potentials.

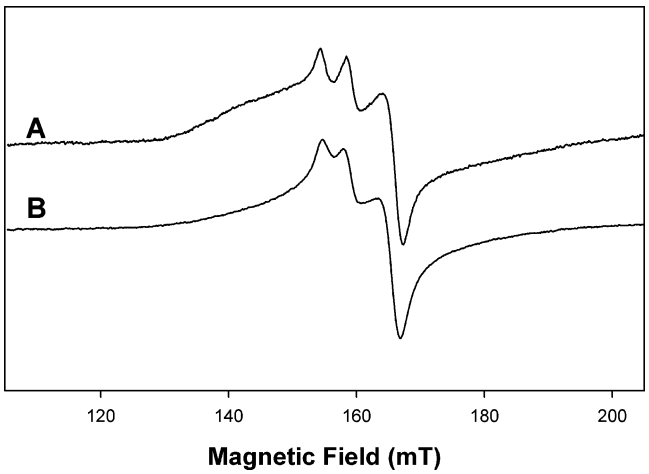

FIGURE 2: EPR spectra of (A) Fe_C/TfR recovered from redox experiment, and (B) free C-lobe. Spectra have been scaled to approximately equal amplitude.

have similar if not identical Fe^{3+} and Fe^{2+} binding constants, and so we take K_d for binding of Fe^{2+} in the complex to be 10^{-3} M as calculated for free Tf (*11*). This value is used to correct the observed redox potentials by accounting for the dissociation of Fe^{2+} that occurs, in both of these systems, upon reduction. In all experiments exposure to air after complete reduction has occurred resulted in reoxidation and regeneration of the Fe(III)-Tf system as judged by EPR and optical spectroscopies.

Redox of Diferric Tf/TfR. The Nernst plots of Figure 3, representing the reduction of Fe^{3+} in the Tf /TfR complex at pH 5.8, were calculated from the amplitudes of the 465 nm peak in the optical spectra, assuming that Fe^{2+} bound to transferrin is incapable of charge-transfer from tyrosinate, and therefore colorless (*2*). Nernst plots corresponding to the raw data are shown in Figure 3A for diferric Tf and diferric Tf/TfR. Three independent determinations are illustrated for diferric Tf/TfR. Figure 3B illustrates the same data, corrected for the dissociation of Fe^{2+} from Tf following a previously described method (*2*). These calculations demonstrate a small consistent shift in the absolute value of the redox potential for both Tf and Tf/TfR as the assumed binding constant for Fe(II) is increased, while the difference in redox potentials for the two systems show little to no change at all. If in fact the Fe(II)-binding constants were

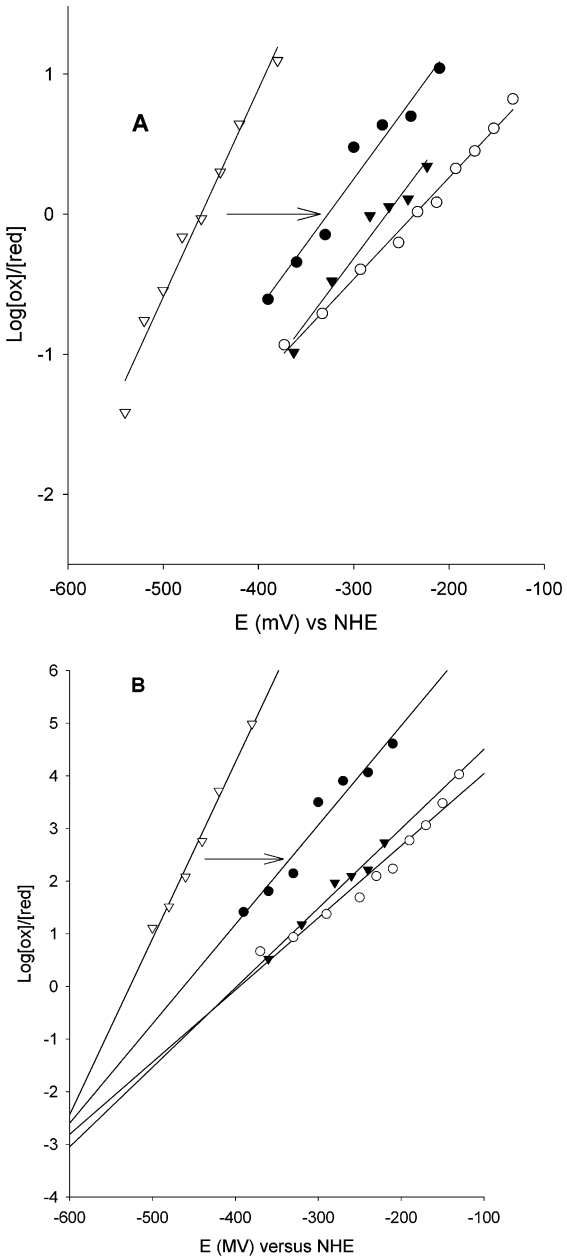

FIGURE 3: (A) Uncorrected Nernst plots for diferric Tf (□) and three independent determinations for diferric Tf/TfR complex (●, ▼, ○). Conditions, and $E_{1/2}$ and n values: (□) Fe_2Tf [Fe(III)] = 0.15(4) mM; pH = 5.8; [Cl^-] = 500 mM. $E_{1/2} = -458$ mV; $n = 0.9$. (●) Fe_2Tf/TfR [Fe(III)] = 0.09 mM; pH = 5.8; [Cl^-] = 500 mM. $E_{1/2} = -327$ mV; $n = 0.5$ (▼) Fe_2Tf/TfR [Fe(III)] = 0.15 mM; pH = 5.8; [Cl^-] = 500 mM. $E_{1/2} = -266$ mV; $n = 0.5$ (○) Fe_2Tf/TfR [Fe(III)] = 0.13 mM; pH = 5.8; [Cl^-] = 500 mM. $E_{1/2} = -233$ mV; $n = 0.4$. (B) Nernst plots corresponding to raw data in part A after correction for Fe^{2+} dissociation from Tf for diferric Tf (□) and three independent determinations for diferric Tf/TfR complex (●, ▼, ○) Corrected $E_{1/2}$ and n values: (□) Fe_2Tf $E_{1/2} = -526$ mV; $n = 1.9$. (●) Fe_2Tf/TfR $E_{1/2} = -462$ mV; $n = 1.1$. (▼) Fe_2Tf/TfR $E_{1/2} = -398$ mV; $n = 0.9$. (○) Fe_2Tf/TfR $E_{1/2} = -395$ mV; $n = 0.8$.

different for Tf and Tf/TfR, then we should have observed a positive shift in $E_{1/2}$ for Tf/Tf-R at pH 7.4 as well, which we did not find.

The diferric Tf/TfR data exhibit complex curvilinear behavior and a linear regression of each data set yields a variable redox potential ($E_{1/2}$). However, for both uncorrected and corrected data the formation of a TfR complex definitively shifts the $E_{1/2}$ significantly positive relative to diferric Tf, as illustrated in Figure 3. We cannot be confident of the cause of the variability of the shift and the curvilinear behavior observed in some cases; release of iron from the N-lobe and scrambling of iron between lobes are likely possibilities. A pronounced differential effect of TfR on the $E_{1/2}$ of Fe^{3+} bound to the C lobe relative to the N lobe is also a likely cause of non-Nernstian behavior. This may also be inferred from the n values (number of electrons in the reduction process) derived from Figure 3B, which vary from 1.9 for diferric Tf and 0.8−1.1 for the diferric Tf/TfR complex. The receptor binding model proposed by Lawrence et al. (*17*) suggests a stronger receptor interaction with C-lobe over N-lobe, confirmed by cell binding studies (*15*), a condition that would also be likely lead to non-Nernstian behavior. Although no simple explanation for the variability of results is at hand, it is clear that $E_{1/2}$ for Tf/TfR is shifted positive relative to diferric transferrin in the absence of receptor, for uncorrected data and for data corrected for dissociation of Fe^{2+} from transferrin.

Redox of C-Lobe/TfR. To contend with the variability of redox results with Tf/TfR complexes, we turned to the monoferric complex of C-lobe with receptor. At pH 7 no reduction is observed down to −370 mV (NHE) in this complex, indicating that the reduction potential is not raised, and may even be lowered, from that displayed by the C-lobe of full-length Tf in the absence of receptor (*2*). Thus, Fe^{3+} in this complex is inaccessible to physiological reductants at the pH where transferrin first encounters TfR. At a pH approximating that of the endosome where iron is released from transferrin, 5.8, however, log(Fe^{3+}-Tf/Fe^{2+}-Tf) is linear with applied potential until reduction is 75−90% complete (Figure 4A,B). Thus, the energy cost of reduction in C-lobe complexed to receptor is greatly decreased by the receptor-induced rise in reduction potential at endosomal pH from −500 to ca. −285 mV, as illustrated in Figure 5.

The corrected $E_{1/2}$ value of ca. −285 mV for $E_{1/2}$ is only as good as the K_d value used to correct for Fe^{2+} dissociation. The value used here and previously (*2*) for K_d is 10^{-3} M (*11*); an increase or decrease in this value by a factor of 10 will shift the corrected $E_{1/2}$ value up or down 50 mV, respectively. However, any change in the K_d value used in the correction will also change $E_{1/2}$ for nonreceptor bound C-lobe in the same manner, consistent with our earlier conclusion that both free and receptor-bound C-lobe have the same Fe^{2+} affinity. This assertion is based on EPR and UV-visible spectral data which demonstrate that receptor binding does not perturb the Fe^{3+} primary coordination shell. Consequently, the positive shift in $E_{1/2}$ reported here for C-lobe when bound to its receptor is independent of the value assumed for K_d. The increase in redox potential makes Fe^{3+} reduction comparable to that of the pyridine nucleotides, −284 mV. Fe^{2+} is bound by transferrin at least 14 orders of magnitude more weakly than Fe^{3+} (*11*), so that reductive release of iron bound to transferrin in the transferrin−transferrin receptor complex is then physiologically and thermodynamically feasible, and the barrier to transport across the endosomal membrane via DMT1 is lifted.

DISCUSSION

Redox events permeate all of iron metabolism. Absorption of non-heme iron largely depends on its oxidation state, with Fe^{2+} strongly favored over Fe^{3+}. During intestinal absorption

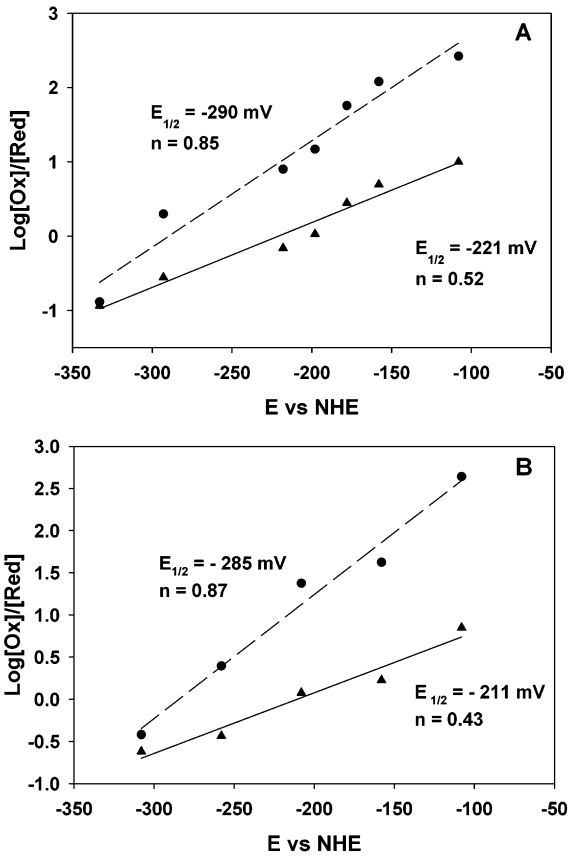

FIGURE 4: Two independent (A and B) representative Nernst plots corresponding to the reduction of Fe^{3+} in the C-lobe/TfR complex. (▲) Raw data; (●) data corrected for Fe^{2+} dissociation from Tf. Conditions (A and B): buffer, 50 mM MES, 500 mM KCl, pH 5.8; [Fe_C/TfR] = 0.19 mM; [MV^{2+}] = 1.4 mM.

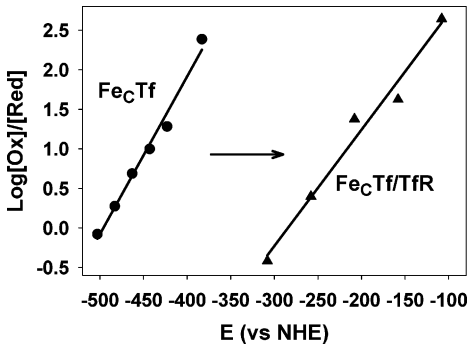

FIGURE 5: Nernst plot for reduction of Fe^{3+} in the C lobe of human transferrin and C-lobe complexed to the transferrin receptor, at endosomal pH 5.8. Data are corrected for Fe^{2+} dissociation. $E_{1/2} = -501 \pm 12$ mV and $n = 1.2 \pm 0.2$ for Fe_CTf. $E_{1/2} = -285 \pm 25$ mV, and $n = 0.87 \pm 0.24$ for Fe_CTf/TfR (The errors in the $E_{1/2}$ and n values are calculated from regression analyses with a 95% confidence level). Conditions: buffer, 50 mM MES, 500 mM KCl, pH 5.8; [Tf C-lobe/TfR] = 0.19 mM; [Fe_CTf] = 0.20 mM.

reduction of Fe^{3+} is accomplished by a duodenal reductase, Dcytb, with reducing equivalents provided by ascorbate (*20*). Export of iron from absorbing (or other) cells entails participation of hephaestin, a multicopper oxidase related to ceruloplasmin and thought to facilitate binding of Fe^{2+} to transferrin by virtue of its ferroxidase activity (*21*). Transport of nontransferrin-bound iron into cells or out of endosomes is accomplished by the divalent metal ion membrane transporter, DMT1, that only accepts Fe^{2+} (*22*). A previously unknown step in intracellular iron metabolism is where and how reduction of transferrin-borne Fe^{3+} takes place. We now offer evidence that this step may occur as a central event in iron release from transferrin.

On the basis of redox studies of free Tf in all of its iron bearing forms, we have previously claimed that reduction of iron is not physiologically feasible unless there is a cascade of reactions involving Fe^{2+} chelation (*2*). Although that claim stands for free Tf, it overlooked the fact that, in its journey through the cell, Tf is always associated with TfR (*5*). We have therefore expanded our earlier redox studies to encompass TfR and its complexes with Tf and the C-lobe of Tf.

Although Nernst plots of Fe^{3+} reduction in native diferric Tf/TfR did not yield straightforward and reproducible results, the consistent indication was that $E_{1/2}$ is significantly shifted to a more positive potential from that for free Tf at pH 5.8, but not at pH 7.4. If verifiable, therefore, the implication would be that physiological reduction of Fe^{3+} is feasible within the endosome bearing Tf/TfR. A reasonable explanation for the experimental difficulties with Tf/TfR is that binding of iron to the N-lobe of Tf is substantially weakened as pH is lowered, so that considerable loss of iron from the lobe occurs at the pH of the redox experiments, 5.8 (some Fe^{2+} dissociation occurs in all of our experiments, but not in sufficient amounts to affect results significantly). The reduction potential of iron freed from transferrin would be expected to be substantially more positive than that of iron bound to transferrin (*7*), consistent with the observed nonlinear Nernstian behavior in the low pH studies of iron in full-length transferrin. Replacement of Tf by single-sited C-lobe circumvented the difficulties, whatever they are, encountered in measuring reduction potentials of two-sited Tf. Nernst plots of Fe^{3+} reduction in C-lobe/TfR are appropriately linear, with slopes in plots corrected for binding of Fe^{2+} to C-lobe yielding n values near 1 (0.85 and 0.87) as expected of a one-electron process (Figure 4). Observed values of applied potential at half reduction (log Fe^{3+}/Fe^{2+} = 0) unequivocally indicate a reduction potential of Fe^{3+} in C-lobe within the range of biological reductants (Figure 4) and formal potentials corrected for Fe^{2+} dissociation are shifted into that range relative to the receptor-free system (Figure 5), as previously discussed.

The mechanism by which interaction of TfR with Tf or C-lobe raises the reduction potential of Fe^{3+}, and therefore lowers the energy cost of reductive release of iron, at endosomal pH, but not at extracellular pH, is not clear. A pH-dependent conformational transition in the soluble Tf-binding exocytic portion of TfR obtained by tryptic digestion, leading to self-association below pH 6.0, has been detected by CD and correlated gel filtration-EM studies (*23*). An attractive possibility, therefore, is that such a change in receptor has a role in raising the reduction potential of Fe^{3+} in transferrin, but the molecular basis for the change is unknown so that its experimental exploration is not yet feasible. A further possibility, that the first coordination sphere of iron in Tf is distorted by a receptor-induced conformational change, is not supported by the unperturbed optical and EPR spectra of the complexes. We therefore consider that the redox potential-raising effect of TfR results from disturbance in the outer coordination sphere of specifically bound iron. In the following model, we assume that the iron ligands remain unchanged and in their native configurations. A difference in TfR affinity for iron-bearing

Scheme 1: Free Energy Cycle for Coupled Transferrin−Transferrin Receptor Binding and Fe^{3+}/Fe^{2+}-Transferrin Redox

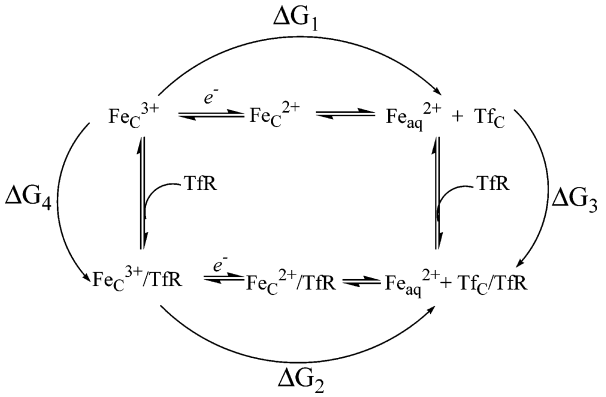

vs iron-free Tf will result in a shift in $E_{1/2}$ between Fe^{3+}Tf and Fe^{3+}Tf/TfR that does not require perturbation of the first coordination shell of Fe^{3+}. Such a difference is supported by reversible stabilization of detergent-solubilized rabbit Tf/TfR complexes in a Tris-citrate buffer at pH 5.0 (*10*), and by the tight binding of human apoTf to HepG2 cells at pH 5.4 (K_d = 13 nM; for comparison, the K_d of diferric Tf at pH 7.4 = 9 nM) without detectable binding at pH 7.4 (*5*). (The strength of TfR-binding by iron-bearing transferrin at low pH has not to our knowledge been quantitatively studied, perhaps because of the confounding effects of iron release in low pH buffers.) The accelerating effect of TfR on iron release from the C-lobe of Tf at pH 5.6, but not at pH 7.4 where an opposite action is observed, is also consistent with the present thermodynamic studies (*14*, *24*).

Consideration of differential receptor binding between apo and holo transferrin at pH 7.4 (plasma) and 5.5 (endosome) provides some insight into the origin of the observed shift in $E_{1/2}$ for Fe^{3+} in C-lobe complexed to TfR (Fe_C/TfR) relative to free C-lobe (Fe_C). This may be assessed through an analysis of a series of coupled equilibria as shown in Scheme 1. ΔG_1 corresponds to our observed $E_{1/2}$ (uncorrected) value for nonreceptor bound Fe_C, or alternatively to our corrected $E_{1/2}$ plus the free energy change associated with an estimated K_d value for Fe^{2+} bound to Tf (*11*). ΔG_2 corresponds to the same processes for receptor bound C-lobe, Fe_C/TfR. Assume initially that Scheme 1 represents the system at endosomal pH 5.5. A differential affinity of TfR for holo-Tf and apo-Tf where the apo form is more tightly held at pH 5.5 means that $\Delta G_3 < \Delta G_4$ and therefore $\Delta G_1 > \Delta G_2$. This suggests that the reduction of receptor-bound C-lobe transferrin is more favored than when not bound to the receptor. Consequently, $E_{1/2}^{FeTf/TfR} > E_{1/2}^{FeTf}$ as we observe for either corrected or uncorrected values. Analysis of Scheme 1 demonstrates that the energy of apo-Tf/TfR binding at pH 5.5 effectively serves to shift the observed $E_{1/2}$ value for FeTf to a more positive (favorable) value relative to that observed in the absence of TfR. At pH 7.4 an enhanced affinity of apo-Tf for TfR over FeTf binding to TfR does not occur, and therefore we do not observe a positive shift in $E_{1/2}$. A coupling of the apo transferrin−transferrin receptor binding energy to the reduction process may be viewed as a second coordination shell effect and is consistent with the lack of perturbation of the UV-vis and EPR spectra on TfR binding, while still influencing $E_{1/2}$.

Although the feasibility of reductive release of iron from the Tf/TfR complex within the endosome of the iron-requiring cell is established, we recognize that physiological reduction of transferrin-borne iron has not been demonstrated. Such reduction, if it occurs, would ultimately have to be driven by intracellular reductants with low potentials because of the low reduction potential of Fe^{3+} in transferrin even in the Tf/TfR complex. A membrane NADPH-dependent enzyme catalyzing Fe^{3+} reduction in yeast, FRE1, has been identified (*25*). FRE1 has similarities to b-type cytochromes and the NADPH oxidase of human leukocytes, and may also carry a flavin group enabling it to engage in one-electron redox reactions. Furthermore, the reduction potential of FRE1, near −250 mV, approaches that of Fe^{3+} in the Tf/TfR complex. Transmembrane transport of iron (and other transition metal ions) in yeast shares many features with mammalian cells, so that a reductive event in release and transmembrane transport of iron from transferrin is not unlikely.

The transferrin receptor is more than a simple conveyor of transferrin and its iron.

REFERENCES

1. Kretchmar, S. A., Reyes, Z. E., and Raymond, K. N. (1988) *Biochim. Biophys. Acta 956*, 85−94.
2. Kraiter, D., Zak, O., Aisen, P., and Crumbliss, A. L. (1998) *Inorg. Chem. 37*, 964−968.
3. Kawabata, H., Yang, S., Hirama, T., Vuong, P. T., Kawano, S., Gombart, A. F., and Koeffler, H. P. (1999) *J. Biol. Chem. 274*, 20826−20832.
4. Klausner, R. D., Ashwell, J. V., VanRenswoude, J. B., Harford, J., and Bridges, K. (1983) *Proc. Natl. Acad. Sci. U.S.A. 80*, 2263−2266.
5. Dautry-Varsat, A., Ciechanover, A., and Lodish, H. F. (1983) *Proc. Natl. Acad. Sci. U.S.A. 80*, 2258−2262.
6. Andrews, N. C., Fleming, M. D., and Gunshin, H. (1999) *Nutr. Rev. 57*, 114−123.
7. Buettner, G. R. (1993) *Arch. Biochem. Biophys. 300*, 535−543.
8. Aisen, P. (1998) Transferrin, its receptor, and the uptake of iron by cells. *Metal Ions Biol. Syst. 35*, 585−631.
9. Katz, J. H. (1961) *J. Clin. Invest. 40*, 2143−2152.
10. Ecarot-Charrier, B., Grey, V. L., Wilczynska, A., and Schulman, H. M. (1980) *Can. J. Biochem. 58*, 418−426.
11. Harris, W. R. (1986) *J. Inorg. Biochem. 27*, 41−52.
12. Swaddle, T. W., and Merbach, A. E. (1981) *Inorg. Chem. 20*, 4212−4216.
13. Grant, M., and Jordan, R. B. (1981) *Inorg. Chem. 20*, 55−60.
14. Bali, P. K., Zak, O., and Aisen, P. (1991) *Biochemistry 30*, 324−328.
15. Zak, O., and Aisen, P. (2002) *Biochemistry 41*, 1647−1653.
16. Zak, O., and Aisen, P. (2003) *Protein Expr. Purif. 28*, 120−124.
17. Lawrence, C. M., Ray, S., Babyonyshev, M., Galluser, R., Borhani, D. W., and Harrison, S. C. (1999) *Science 286*, 779−782.
18. Lebrón, J. A., Bennett, M. J., Vaughn, D. E., Chirino, A. J., Snow, P. M., Mintier, G. A., Feder, J. N., and Bjorkman, P. J. (1998) *Cell 93*, 111−123.
19. Grady, J. K., Mason, A. B., Woodworth, R. C., and Chasteen, N. D. (1995) *Biochem. J. 309*, 403−410.
20. McKie, A. T., Latunde-Dada, G., Miret, S., McGregor, J. A., Anderson, G. J., Vulpe, C. D., Wrigglesworth, J. M., and Simpson, R. J. (2002) *Biochem. Soc. Trans. 30*, 722−724.
21. Vulpe, C. D., Kuo, Y. M., Murphy, T. L., Cowley, L., Askwith, C., Libina, N., Gitschier, J., and Anderson, G. J. (1999) *Nat. Genet. 21*, 195−199.
22. Andrews, N. C. (1999) *Int. J. Biochem. Cell Biol. 31*, 991−994.
23. Turkewitz, A. P., Schwartz, A. L., and Harrison, S. C. (1988) *J. Biol. Chem. 263*, 16309−16315.
24. Bali, P. K., and Aisen, P. (1991) *Biochemistry 30*, 9947−9952.
25. Shatwell, K. P., Dancis, A., Cross, A. R., Klausner, R. D., and Segal, A. W. (1996) *J. Biol. Chem. 271*, 14240−14244.

BI0353631